Hybrid Elliptic TEM Horn with Symmetric Main Beam

J.A.G. Malherbe, *Life Fellow*, IEEE
Department of Electrical, Electronic and Computer Engineering
University of Pretoria
Pretoria, South Africa
jagm@up.ac.za

Abstract - **The structure of a TEM horn with new plate separation and width profiles is described. It is shown that the combination of a superellipse for the separation function, and a new function for the pate width, results in a horn with nominally frequency-independent properties to beyond 42 GHz. The new separation function has elliptic properties at the throat of the horn, and gradually opens to an almost linear taper.**

Keywords- TEM horn; superelliptic horn profile

I INTRODUCTION

Previously [1] it was found that the radiation properties of TEM horns can, to a certain extent, be controlled by varying the flare as well as the plate width of the horn [2]. It was also shown that the popular approach to the plate width specification of choosing some form of impedance match, is not valid. The important variable is to ensure mode matching between the feed and free space.

In [3], the plate separation was described by a superellipse, which made it possible to separately control the dimensions in the throat and those in the vicinity of the aperture of the horn. This in turn made it possible to have some measure of control over the high frequency performance as compared to the low frequency properties.

A number of authors have recently proposed a variety of new horn structures. Different aperture impedances, combined with a linear horn, are investigated in [4], while in [5], a binomial impedance taper is compared to an exponential, Klopfenstein and triangular taper; in [6], a Hecken taper is combined with a number of different aperture impedances. A modification of the aperture edge in order to improve the radiation pattern properties is proposed in [7]; this was previously analytically treated in [8].

In this paper, a superelliptic plate separation function is employed; this is combined with a new function, in which a modified superelliptic function is employed for calculating the plate width. It is shown that this results in a structure that exhibits extreme wideband and frequency independent radiation properties. The structure is analyzed numerically and gain, *VSWR* and radiation properties are presented.

II HYBRID ELLIPTIC HORN STRUCTURE

A. Parallel Line Feed

The TEM horn described here is a balanced parallel plate structure. The plates of the feed line are spaced 1.0 mm, and 5.9 mm wide, for a 50 Ω characteristic impedance.

A balun for feeding the structure is not considered in the analysis; previously [9] the design described in [10] was used with success. Alternatively, the method described in [11] can be applied. It is, however, important to eliminate the effects of the feed point in the numerical analysis. To that end, a back-to-back feed was evaluated and it was ensured that it does not contribute to the input impedance performance of the antenna; Fig. 1 shows the VSWR of the feed. This will later be compared to the corresponding properties of the feed plus antenna.

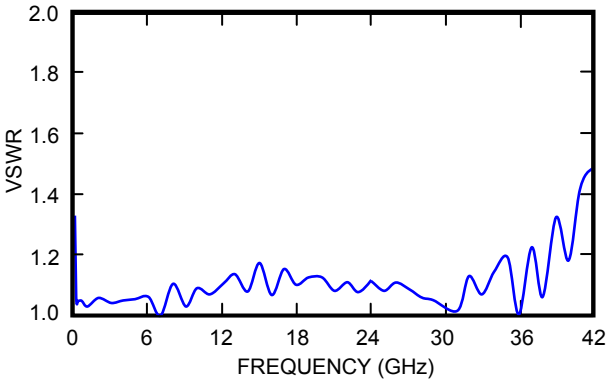

Figure 1. *VSWR* of numerically modelled parallel plate feed.

B. Horn Parameters

The general description of an ellipse in parametric form is given by

$$\left.\begin{aligned} u(\vartheta) &= a(\cos\vartheta)^{2/m} \\ v(\vartheta) &= b(\sin\vartheta)^{2/n} \end{aligned}\right\} m,n>0. \qquad (1)$$

For $m, n < 2$, the function is a hypoellipse; for $m, n > 2$, a hyperellipse; and for $m = n = 2$ a standard ellipse. The major and minor axes are a and b, and ϑ is the parameter. The general shape of these functions are illustrated in Fig. 2

978-1-4673-0292-0/12/$31.00 ©2012 IEEE

for different values of m, n; only the first quadrant, $0 \le \vartheta \le \pi/2$, is relevant. In Fig. 2, the values $\vartheta = 0$ and $\vartheta = \pi/2$ are shown; however, note that ϑ is not the angle between (u,v) and the u-axis.

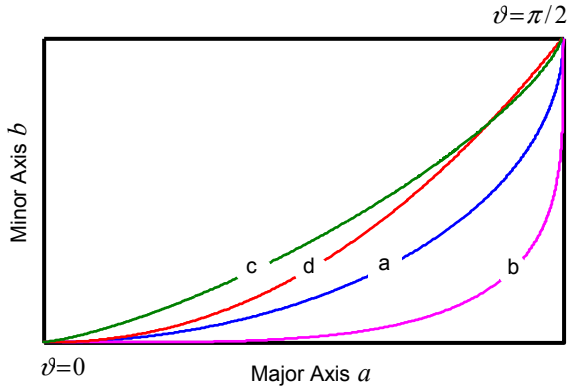

Figure 2. Ellipses. a: $m = n = 2$, b: $m = n = 4$; c: $m = n = 1.5$; d: modified superellipse.

Through application of different powers of m, n, various profiles can be achieved. The aim is to shape the E- and H-plane patterns to be congruent, as well as to obtain as little variation with frequency as possible. In this way the main beam of radiation will be symmetrical, and the gain response *vs* frequency flat.

1) Plate separation function: To this end, a plate separation function similar to that used in [3], was employed, with a slight increase in the rate of separation at the aperture.

$$x(t) = 480 \sin^{1.4} \vartheta \tag{2}$$

$$z(t) = 120.5 - 120 \cos^{0.7} \vartheta = 120(1 - \cos^{0.7} \vartheta) + 0.5 \tag{3}$$

The function has hypoelliptical properties in the axial direction and hyperelliptical properties in separation. The plates are separated 1 mm at the throat, and 241 mm at the aperture, while the total length of the horn is 480 mm, as shown in Fig. 3. Note the format for the expression for $z(t)$; this is to ensure that the correct branch of the hyperellipse is used.

2) Plate width function: In order to control the radiation properties in the H-plane, it is necessary to employ a function that is smooth at the throat of the horn, with typical elliptic properties, but is wider at both the middle and the aperture of the horn than the standard ellipse, while maintaining continuity of the profile. This would contract the H-plane radiation patterns to more closely map onto the E-plane patterns.

By choice of m = 0.5, the width of the horn increases almost linearly towards the aperture of the horn. However, the change in width is too rapid at the throat, and consequently the whole of the parametric function was raised by an additional power of 1.5. This ensures that the width changes very slowly at the throat, approximating that of an ellipse for small ϑ, while maintaining a linear profile as the aperture is approached. The width function is given by (4) and (5).

$$x(t) = 480 \sin^{1.4} \vartheta, \tag{4}$$

$$y(t) = 85(1 - \cos^{2.0} \vartheta)^{1.5} + 2.95. \tag{5}$$

This function is shown in Fig. 2(d); note that the function is smooth at $\vartheta = 0$, but that discontinuous at $\vartheta = \pi/2$. Fig. 3 shows the geometry of the horn. The plates are 5.9 mm wide at the throat, and 176 mm at the aperture.

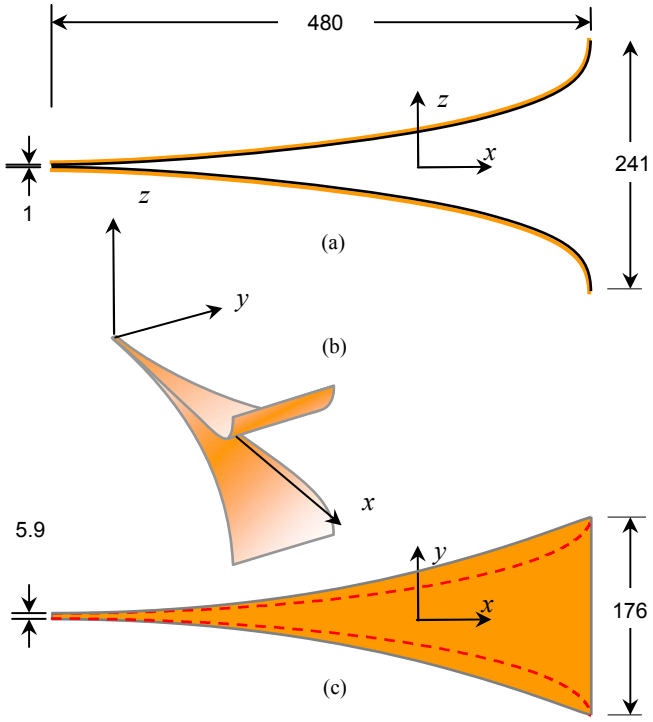

Figure 3. Horn dimensions and profiles. (a) Separation; (b) oblique view; (c) width. The dashed profile in (c) is that of a conventional ellipse.

III Calculated Performance

The radiation and impedance performance of the horn were calculated using FEKO [12], over the frequency band 100 MHz to 42 GHz. The gain *vs* frequency response is shown in Fig. 4, while the input impedance and VSWR is shown in Fig. 5. Fig. 6 is an expanded plot of the impedance between 100 MHz and 3 GHz.

Fig. 7(a) shows the E- and H-plane radiation patterns for 250 and 700 MHz, respectively, while the patterns for 2 and 6 GHz are shown in Fig. 7(b). Similar sets of radiation patterns for 6, 12, 18, 24, 30, 36 and 42 GHz are shown in Figs 8(a) to 8(g). In Fig 9(a) all the E-plane radiation patterns from 6 to 42 GHz are plotted overlaying each other, and the same is done for the H-plane patterns in Fig. 9(b).

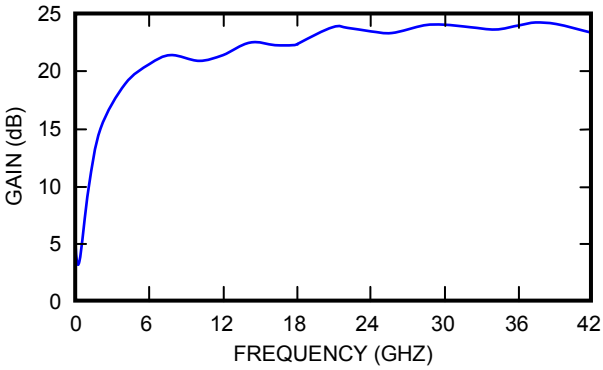

Figure 4. Gain *vs* frequency response.

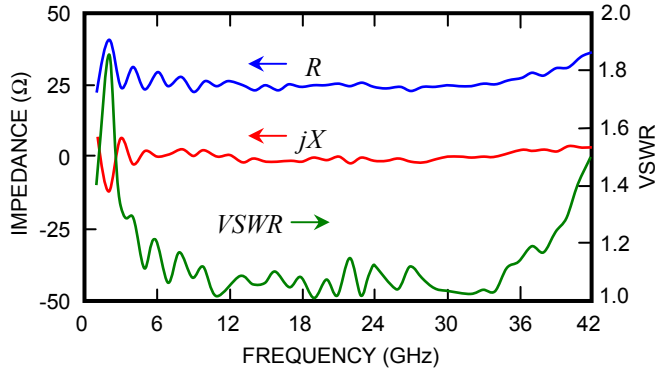

Figure 5. Variation of Impedance and VSWR with frequency.

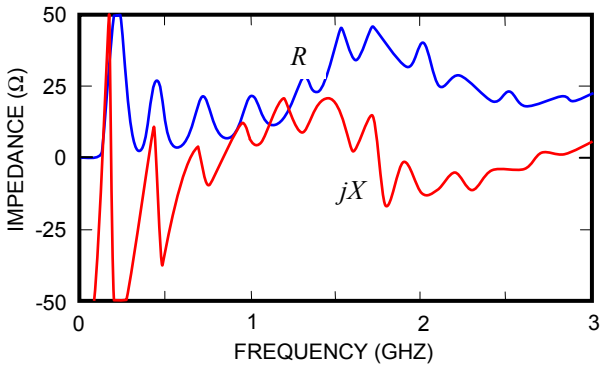

Figure 6. Expanded impedance response.

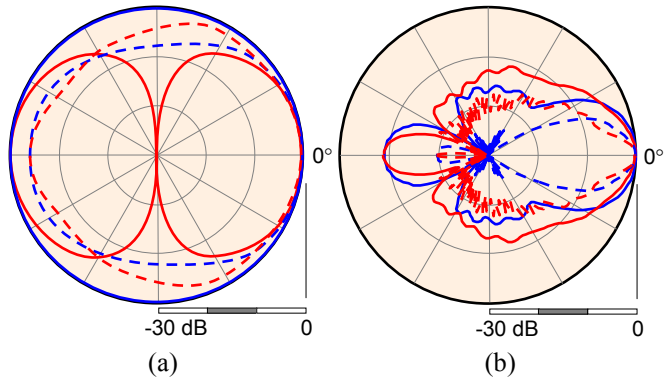

Figure 7. (a) E-(red) and H- (blue) plane radiation patterns for 250 (——) and 700 MHz (- - -), and (b), 2 (——) and 6 GHz (- - -).

Fig. 10 shows the 3-D radiation pattern at 42 GHz.

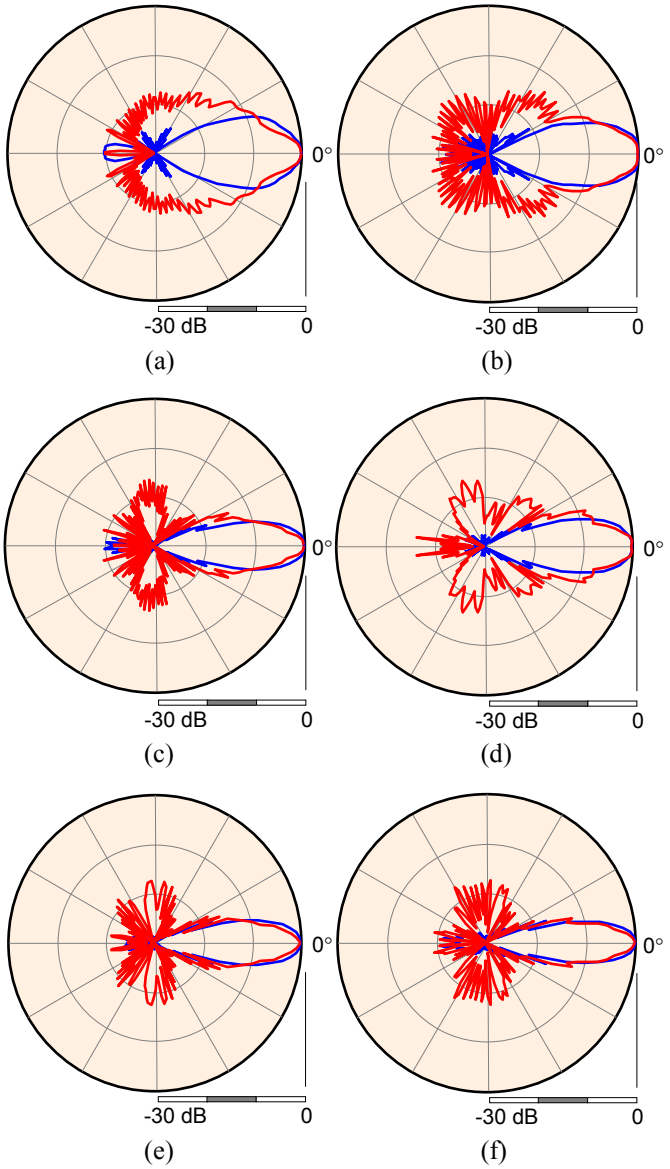

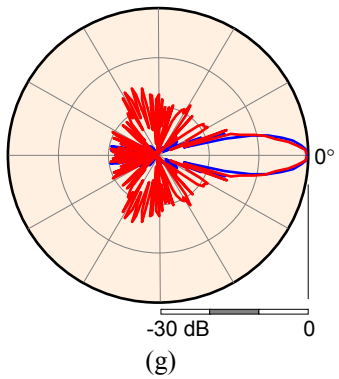

Figure 8. E-(red) and H- (blue) plane radiation patterns for 6, 12, 18, 24, 30, 36 and 42 GHz shown in (a) to (g) respectively.

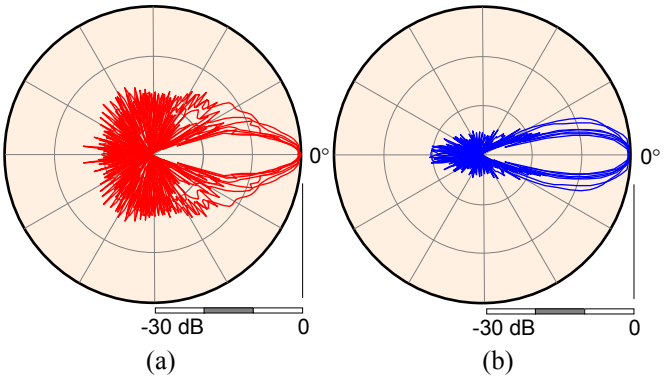

Figure 9. Overlaid radiation patterns. (a) E-plane and (b) H- plane.

IV Discussion

The proposed horn has an impedance bandwidth that stretches from 250 MHz to 42 GHz, the VSWR lying well below 2, as seen in Fig. 5. However, the gain only rises to within 3 dB of its maximum of 24.5 dB at about 6 GHz. A study of the radiation patterns up to 6 GHz reveals that a main beam has not yet formed at the lower frequencies. In fact, this corresponds to the so-called dipole region [13] as can also be very clearly seen from the expanded impedance response of Fig. 6.

The oscillations evident in Fig. 6 correspond to multiple half wavelength resonances of the horn structure, if the length is measured along the curve of the horn plates; the first resonance occurs at almost exactly the frequency where the total plate length is λ/2. Many of the extremely wideband claims found in the literature refer only to the impedance bandwidth and neglects the fact the horn radiates rather poorly at the lower frequencies.

The region between 1 and 6 GHz corresponds to the resonant part of the horn, where standing waves are formed between the horn throat and the aperture. It is similarly characterized by fairly rapidly changing gain, and Fig. 7(b) shows how the radiation patterns are starting to form. As such, these regions are characteristic of all TEM horns and a function of the length of the horn.

V Conclusion

The proposed horn can be considered to be functional above 6 GHz. Performance beyond 42 GHz will only be limited by the practical realization of the structure and the ability to construct a balun of sufficient bandwidth. Over this entire frequency band, the E- and H-plane patterns are almost identical up to the -6 dB points; furthermore, there is little variation with frequency beyond about 12 GHz.

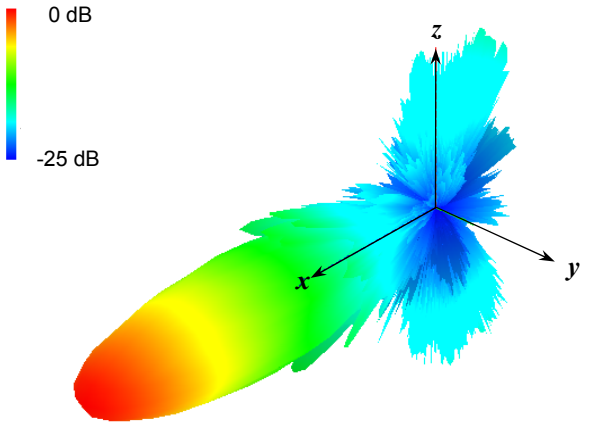

Figure 10. 3-D radiation pattern at 36 GHz.

References

[1] J.A.G. Malherbe, “Frequency-Independent Performance of Elliptic Profile TEM Horns,” Microwave Opt. Technol. Lett., vol. 51, no. 3, pp. 607-612, March 2009.

[2] J.A.G. Malherbe, “Width profile of TEM elliptic horns,” in XII Int. Symp. Microwave and Opt.Technol. (ISMOT-2009), New Delhi, India, Dec. 16 – 19, 2009, pp. 555-558. (Invited paper).

[3] J.A.G. Malherbe, “Superelliptic TEM Horn,” in Proc. 40th European Microwave Conf., 28-30 Sept. 2010, Paris, France, pp. 735-738.

[4] A. Zhang, L. Wang, C. Guo and Y. Jiang, “Constant Impedance TEM Horn Antenna: Aperture and Characteristic Impedance’s Impacts on Axial Electric Field,” Jnl. Infrared, Millimeter and Terahertz Waves, vol. 30, no. 10, pp. 1067-1072, 2009.

[5] M. Khorshidi and M. Kamyab, "New exponential TEM horn antenna with binomial impedance taper," Int. J.Electron.Commun. (AEU), vol. 64, no. 11, pp. 1073 – 1077, Nov. 2010.

[6] C-P. Kao, J. Li, R. Liu, and Y. Cai, "Design and Analysis of UWB TEM Horn Antenna for Ground Penetrating Radar Applications," IEEE IGARSS 2008, pp. IV-569 –IV-572.

[7] F. Karshenas, A. R. Mallahzadeh, and A. Imani, "Modified TEM Horn Antenna for Wideband Applications," in 13th Int. Sym. Antenna Techno. App. Electromagn. and Canadian Radio Sci. Meeting, 2009.

[8] J.W. Odendaal and C.W. I. Pistorius, "E-Plane Analysis of a Modified Horn Antenna with Suppressed Far-out Sidelobe Level," IEEE Tans. Antennas Propagat.., vol. 40, no. 6, pp. 620-627, June 1992.

[9] J.A.G. Malherbe, “Extreme Performance TEM Horn,” Microwave Opt. Technol. Lett. Vol. 50, No. 8, pp. 2121-2125, Aug. 2008.

[10] M. Manteghi and Y. Rahmat-Samii, "A novel UWB feeding mechanism for the TEM horn antenna, reflector IRA, and the Vivaldi antenna," IEEE Antennas Propagat. Mag. vol. 46, no. 4, pp. 81–87, Oct, 2004.

[11] S. Ghosh, B.K. Sarkar and S.V. Pandey, "TEM Horn Antenna using Improved UWB Feeding Mechanism," in Proc. 38th European Microwave Conf., October 2008, Amsterdam, pp. 1398 – 1401.

[12] FEKO, EM Software & Systems-S.A. (Pty) Ltd. Available at http://www.feko.info/index.html.

[13] JAG Malherbe, “Design of Ultra Wideband TEM Horns,” in 2007 Asia Pacific Microwave Conf., APMC 2007, Bangkok, Thailand, 11-15 Dec. 2007, pp. 449-452.